Production of Sc nuclides in the interaction of ^{238}U with 1–300 GeV protons*

Ø. Scheidemann† and N. T. Porile
Department of Chemistry, Purdue University, Lafayette, Indiana 47907
(Received 9 February 1976)

Cross sections and thick-target recoil properties of several Sc nuclides formed in the interaction of ^{238}U with 1–300 GeV protons have been determined. The ranges of all the products decrease markedly between 1 and 10 GeV and only slightly thereafter. The forward-to-backward emission ratios peak at 3 GeV and decrease to a value of unity at 300 GeV. The excitation functions increase sharply up to ~ 10 GeV and go through a very shallow peak at this energy. The results are analyzed within the context of the two-step model of high-energy reactions and found to require a larger ratio of transverse to forward momentum transfer than expected on this basis. The emission of an excited hadron in the cascade can also account for the data. The systematics of fragment momenta are developed.

[NUCLEAR REACTIONS Measured σ, $2W(F+B)$, and F/B of various Sc nuclides formed in interaction of ^{238}U with 1–300 GeV protons.]

I. INTRODUCTION

The energy dependence of the recoil properties of deep spallation and fission products formed in the interaction of ^{238}U with GeV protons was first investigated by Beg and Porile[1]. These workers found that the ratio of forward-to-backward emission (F/B) of the deep spallation products (e.g. ^{131}Ba and ^{83}Sr) went through a sharp peak at 2–3 GeV while the ranges decreased by about a factor-of-two over a somewhat wider energy interval (~ 1–4 GeV). On the other hand, the ranges and F/B values of the fission products were found to be nearly independent of bombarding energy. Earlier work[2–7] had already established that the ranges of deep spallation products at 6 or 18 GeV were substantially lower than those obtained below 1 GeV.

Beg and Porile[1] interpreted these results in terms of a transition from a binary fission process to fragmentation. They were able to obtain qualitative agreement with the recoil properties of deep spallation products measured at bombarding energies above 4 GeV by means of a cascade-evaporation calculation modified to include fragment emission. The properties of the emitted fragments were based on the differential range and angular distribution measurements[8] of ^{24}Na formed in the interaction of 2.9 GeV protons with ^{209}Bi. The presumed connection between deep spallation and fragmentation has made it of interest to measure the energy dependence of the recoil properties of light fragments in order to ascertain whether they are in concordance with those of the deep spallation products. Kaufman and Weisfield[9] recently determined the recoil properties of ^{24}Na and ^{28}Mg from the interaction of ^{238}U and ^{197}Au with 3–300 GeV protons. We present here the results of cross-section and recoil measurements on somewhat heavier fragments, scandium isotopes formed in the interaction of ^{238}U with 1–300 GeV protons.

II. EXPERIMENTAL

The general procedure for the simultaneous determination of cross sections and thick-target recoil properties has been described in previous reports from this laboratory[10,11]. Target stacks were irradiated in the circulating beam of the zero gradient synchrotron (ZGS) with 1.0–11.5 GeV protons, in that of the alternating gradient synchrotron (AGS) with 28.5 GeV protons, and in the meson hall at Fermilab with 300 GeV protons. The target stacks consisted of a 20 μm thick depleted uranium foil surrounded by three pairs of 20 μm thick aluminum foils. The inner pair served as recoil catchers, the middle pair as beam monitors, and the outer pair as guard foils. All the foils were carefully aligned to insure that they intercepted the same number of protons. We have previously established that under these conditions the loss of recoils from the target edge is negligibly small. Since the Fermilab irradiations were performed in an open air section of an external beam line the target stack was sealed in an evacuated plastic bag.

Following irradiation the target and catcher foils were separately dissolved and scandium separated by adaptation of standard radiochemical procedures[12]. The various samples were assayed with a calibrated Ge(Li) detector operated in conjunction with a 4096 channel analyzer equipped with magnetic tape readout. Table I summarizes the decay properties of the observed Sc nuclides. Portions of the γ-ray spectra containing the peaks of interest were analyzed with the code SAMPO[13] in order to obtain the disintegration rates of the nuclides of interest. Each sample from a given experiment was

TABLE I. Decay properties of observed Sc nuclides.

Nuclide	Half-life	γ-ray (keV)	Branching ratio[a] %
^{44}Sc^{m}	2.44d	271.4	86.0
^{46}Sc	83.9d	889.3	100
		1120.5	100
^{47}Sc	3.35d	159.4	70.0
^{48}Sc	1.82d	983.3	100
		1037.4	98.0
		1311.7	100

[a]"Nuclear Level Schemes," Nuclear Data Group, ed. Academic Press, New York, 1973.

TABLE II. Cross sections (mb) for the independent formation of Sc isotopes in the interaction of ^{238}U with high-energy protons.

E_p (GeV)	$^{44}Sc^m$	^{46}Sc	^{47}Sc	^{48}Sc
1.0	(6.48±0.45)x10^{-2}	0.641±0.043	0.885±0.054	0.748±0.039
2.0	0.307±0.017	2.08±0.12	2.28±0.12	1.71±0.09
2.15	0.429±0.023	2.64±0.13	2.95±0.16	2.08±0.10
3.0	0.646±0.039	3.79±0.24	3.45±0.20	2.37±0.13
4.0	0.905±0.056	4.85±0.25	4.21±0.27	2.81±0.15
6.0	1.24±0.08	6.15±0.35	5.09±0.42	3.28±0.29
11.5	1.92±0.12	7.22±0.39	6.91±0.47	3.99±0.23
28.5	1.74±0.10	6.32±0.32	6.06±0.31	3.24±0.16
300	1.81±0.13	6.92±0.46	6.16±0.31	3.57±0.19

assayed at least two times and the resulting disintegration rates, extrapolated to the end of bombardment, were averaged using the reciprocals of the variances obtained from SAMPO as the weighting factors. The activity measurements were usually performed in a high geometry configuration. In order to check for possible reductions in photopeak efficiency due to summing effects, measurements were also performed for a 10 cm sample-to-detector distance. It was found that only ^{48}Sc, which has three intense γ-rays in coincidence, required correction. The magnitude of this effect was found to be 13%.

The beam intensity was determined by means of the $^{27}Al(p,3pn)$ monitor reaction. The disintegration rate of ^{24}Na was determined in the same manner as those of the nuclides of interest. The cross section of this reaction decreases from 10.5 mb at 1 GeV to 8.6 mb at 11.5 GeV[14] and remains invariant at higher energies[15].

III. RESULTS

The cross sections, experimental ranges, and F/B values of the various Sc nuclides are tabulated in Tables II - IV, respectively. The experimental range in the target material is defined as 2W(F+B) mg/cm^2, where W is the target thickness and F and B are the fractional number of product nuclides recoiling into the forward and backward catcher, respectively. The ranges have been reduced by 6% to correct for scattering at the target-catcher interface[16]. All the results are the weighted averages of two or more replicate determinations excepting those at 2.0 and 2.15 GeV, which are based on single experiments. As there appears to be a statistically significant difference between some of the results obtained at these two energies we have chosen to present the data separately in spite of the small energy difference. The listed uncertainties are based on those in the γ-ray intensities as obtained from the SAMPO code or on the difference between replicate determinations, if larger. We have in addition included a 3% uncertainty for chemical yield determinations and in the case of the cross sections, a 5% uncertainty in absolute detector efficiency.

The cross sections and recoil properties of $^{44}Sc^m$, ^{46}Sc, and ^{48}Sc refer to the independent formation of these nuclides. The results for ^{47}Sc include a contribution due to the decay of ^{47}Ca. In view of the fact that the separation time was small compared to the ^{47}Ca half-life and since the yield of neutron-excessive ^{47}Ca must be smaller than that of ^{47}Sc we can place an upper limit of 5% on the contribution of ^{47}Ca to the ^{47}Sc data. The excitation functions for the formation of the various Sc isotopes are plotted in Fig. 1. The energy dependence of the recoil ranges and F/B values is shown in Figs. 2 and 3, respectively.

A number of measurements on the formation of Sc nuclides in the interaction of ^{238}U with GeV energy protons have been reported previously. Friedlander and Yaffe[17] measured the cross sections for

TABLE III. Experimental recoil ranges (2W(F+B)) of Sc isotopes. The units are mg/cm^2 of uranium.

E_p (GeV)	$^{44}Sc^m$	^{46}Sc	^{47}Sc	^{48}Sc
1.0	15.38±1.49	17.03±0.91	15.59±1.58	14.29±0.22
2.0	13.73±0.31	13.80±0.52	13.64±0.16	13.29±0.12
2.15	12.54±0.49	11.88±0.79	12.48±0.27	12.45±0.20
3.0	11.17±0.40	10.26±0.57	11.19±0.42	10.94±0.35
4.0	11.55±0.20	11.28±0.16	11.91±0.31	11.59±0.10
6.0	10.17±0.29	10.52±0.34	10.51±0.66	10.16±0.26
11.5	9.30±0.35	8.95±0.29	9.42±0.57	9.57±0.26
28.5	8.69±0.23	9.21±0.15	9.22±0.35	9.85±0.23
300	8.11±0.22	8.87±0.60	8.91±0.38	9.21±0.19

TABLE IV. F/B values for Sc isotopes.

E_p (GeV)	$^{44}Sc^m$	^{46}Sc	^{47}Sc	^{48}Sc
1.0	1.35±0.09	1.29±0.12	1.23±0.08	1.34±0.03
2.0	1.60±0.03	1.58±0.11	1.51±0.02	1.47±0.02
2.15	1.83±0.11	1.48±0.17	1.56±0.05	1.50±0.04
3.0	1.76±0.06	1.78±0.08	1.65±0.03	1.58±0.03
4.0	1.62±0.02	1.48±0.03	1.49±0.02	1.45±0.02
6.0	1.54±0.04	1.40±0.06	1.38±0.04	1.36±0.01
11.5	1.23±0.04	1.27±0.02	1.21±0.04	1.23±0.01
28.5	1.12±0.01	1.10±0.02	1.13±0.03	1.12±0.01
300	1.03±0.02	1.03±0.03	1.02±0.01	1.03±0.01

the production of several Sc nuclides at 3 GeV and Chu[18] performed similar measurements at 28 GeV. Ravn[19] determined both cross sections and thick-target recoil properties at 18 GeV. The results for ^{48}Sc and ^{47}Sc, which are typical of all the data, are compared with the present values in Table V after adjustment for differences in the monitor cross section. It is seen that all the previously determined cross sections are in agreement with the present determinations. However the ranges and F/B determined by Ravn[19] are uniformly lower than our values. The discrepancy is particularly serious for the F/B ratios. Ravn's values are actually less than unity and must be regarded with suspicion.

The measured recoil properties may be used to obtain the corresponding recoil parameters by means of the velocity vector model[16,20,21] embodying the two-step mechanism commonly invoked in high-energy reactions. According to this model the observed velocity of a recoil product $\vec{v}_\ell$ is resolved into components $\vec{v}$ and $\vec{V}$ corresponding to the cascade and deexcitation or breakup steps of the reaction, respectively. The component of $\vec{v}$ parallel to the beam direction is designated $v_\parallel$ and the ratio of its magnitude to that of the breakup velocity is denoted as $\eta_\parallel$. The breakup velocity must by symmetric in the moving system and is in fact assumed to be isotropic. Furthermore, if the range of a recoil in the target material R_ℓ can be related to its velocity by an expression of the form

$$R_\ell = \text{const} \times v_\ell^N \qquad (1)$$

where N is a constant, the following relations can be derived:

$$2W(F+B) = R_o \left[1 + \tfrac{1}{4}\eta_\parallel^{\,2}(N+1)^2\right] \qquad (2)$$

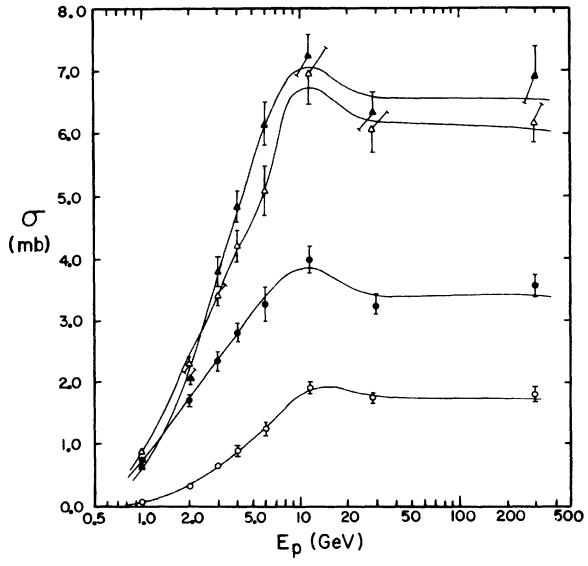

FIG. 1. Excitation functions for the formation of Sc nuclides in the interaction of ^{238}U with high-energy protons. o, $^{44}Sc^m$; ▲, ^{46}Sc; Δ, ^{47}Sc; ●, ^{48}Sc.

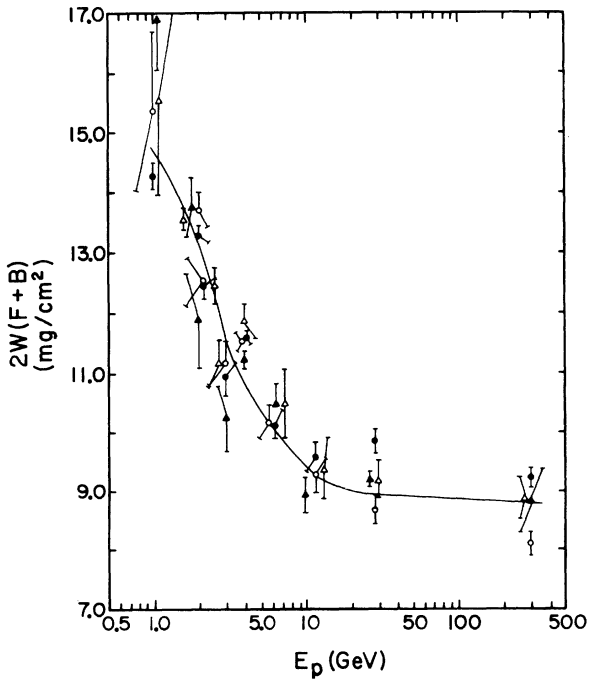

FIG. 2. Energy dependence of recoil ranges of Sc nuclides. The symbols have the same meaning as in Fig. 1. The curve represents the average behavior of the various nuclides. Some of the points have been displaced in energy for greater clarity.

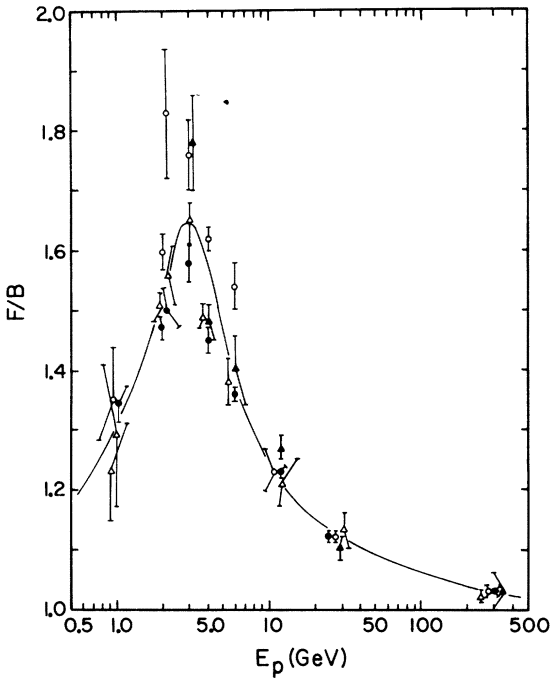

FIG. 3. Energy dependence of F/B ratios of Sc nuclides. See Fig. 2 for details.

and

$$\frac{F}{B} = \frac{1 + \frac{2}{3}\eta_{\parallel}(N+2) + \frac{1}{4}\eta_{\parallel}^2(N+1)^2}{1 - \frac{2}{3}\eta_{\parallel}(N+2) + \frac{1}{4}\eta_{\parallel}^2(N+1)^2} \qquad (3)$$

The quantity R_o is the mean range in the target material corresponding to the recoil speed V. It is possible to obtain V as well as the mean kinetic energy T acquired by the observed products in the deexcitation step from R_o by means of a range-energy relation cast in the form of Eq. (1). We have used the relation developed by Cumming[22] on the basis of the tables of path lengths given by Northcliffe and Schilling[23] coupled with a semi-empirical correction for the difference between path length and projected range. The values of V and $\eta_{\parallel}$ may be used to obtain those of $v_{\parallel}$ and the latter may in turn be used to determine the average cascade deposition energy[21,24], E^*. The relation between E^* and $v_{\parallel}$ may be written as

$$E^* = 3.253 \times 10^{-2}\, k\, A_T\, v_{\parallel}^2\, [T_p/(T_p + 2)]^{1/2} \qquad (4)$$

where E^* and the bombarding energy T_p are expressed in terms of $m_p c^2$, A_T is the target mass in amu and $v_{\parallel}$ is in units of $(\mathrm{MeV/amu})^{1/2}$. The constant k has been evaluated by Porile[24] on the basis of 1.8 GeV Monte Carlo cascade calculations[25] as ∿0.8. The Turkevich two-nucleon collision model, which will be applied to the data in a subsequent section, yields k = 1. In order to maintain consistency with this model we have evaluated E^* assuming k = 1.

The above analysis is based on a number of assumptions and approximations which are fully discussed elsewhere[26] and which can in general lead to ∿ 5% uncertainties in the results. However, in those instances where there is considerable overlap between the $v_{\parallel}$ and V distributions the values of $v_{\parallel}$, and hence those of E^*, can be underestimated by perhaps as much as 25%[27]. Table VI summarizes the values of T, $v_{\parallel}$, and E^* obtained by means of this analysis for $^{44}Sc^m$ and ^{48}Sc. The results for the other Sc isotopes generally lie between those for the above two nuclides.

IV. DISCUSSION

A. Ranges and Momenta of Fragments

The ranges of the various Sc nuclides exhibit a rather similar energy dependence, as shown in Fig. 2. The mean range decreases from a value of 14.5±0.7 mg/cm² at 1 GeV to 9.3±0.3 mg/cm² at 11.5 GeV. Beyond this energy the ranges decrease only slightly to a value of 8.8±0.5 mg/cm² at 300 GeV. This behavior is qualitatively similar to that observed[1] for heavier deep spallation products such as ^{83}Sr or ^{131}Ba although the decrease in magnitude is less pronounced and appears to occur over a wider energy interval. On the other hand, the observed dropoff is substantially greater than it is for lighter products[9] such as ^{24}Na or ^{28}Mg.

It is of interest to compare the energy dependence of the ranges of neutron-deficient and neutron-excessive Sc nuclides. This is most conveniently done in Figure 4 where the ratio of the ranges of $^{44}Sc^m$ and ^{48}Sc is plotted as a function

TABLE V. Comparisons of Sc data with previously reported values (subscripted lit in table).

Nuclide	E_p (GeV)	σ_{lit} (mb)	$\sigma_{present}$ (mb)	F/B_{lit}	$F/B_{present}$	$2W(F+B)_{lit}$	$2W(F+B)_{present}$
^{48}Sc	3.0[a]	4.2±1.7	2.4±0.1				
	18 [b]	3.6±0.1	3.6±0.2	0.94±.02	1.18±.01	8.9±0.2	9.7±0.2
	28 [c]	3.1±0.2	3.2±0.2				
^{47}Sc	3.0[a]	3.0±1.2	3.4±0.2				
	18 [b]	6.2±0.2	6.5±0.4	0.99±.02	1.17±.04	8.8±0.2	9.3±0.4
	28 [c]	6.0±0.5	6.1±0.3				

a. Reference 17
b. Reference 19
c. Reference 18

TABLE VI. Recoil parameters of $^{44}Sc^{m}$ and ^{48}Sc.

E_p (GeV)	T (MeV)	$^{44}Sc^{m}$ $v_{\parallel}$ $(MeV/amu)^{1/2}$	E^* (MeV)	T (MeV)	^{48}Sc $v_{\parallel}$ $(MeV/amu)^{1/2}$	E^* (MeV)
1.0	115±12	.136±.031	582±133	102±2	.123±.009	526±41
2.0	100±3	.203±.008	1060±44	92.8±1.0	.157±.006	819±29
2.15	88.8±4.2	.246±.025	1304±133	85.4±1.7	.158±.010	842±56
3.0	77.3±3.4	.218±.014	1245±80	72.3±3.0	.167±.008	950±44
4.0	81.2±1.8	.191±.005	1146±32	78.3±0.8	.139±.005	834±31
6.0	69.8±2.5	.160±.010	1016±63	66.6±2.1	.108±.003	683±20
11.5	63.1±3.0	.0734±.0017	495±78	61.8±2.1	.0699±.0030	471±20
28.5	58.1±2.0	.0386±.0031	271±22	64.4±2.0	.0391±.0031	275±22
300	53.3±1.9	$(9.72\pm6.39)\times10^{-3}$	71±47	59.1±1.6	$(9.86\pm3.24)\times10^{-3}$	72±24

of energy and compared with similar ratios for ^{67}Ga and ^{73}Ga [ref. 28] as well as ^{83}Sr and ^{91}Sr [refs. 1, 29]. The range ratio for Sc nuclides shows little variation with energy although there does appear to be a statistically significant decrease of ∿ 15% between 1 and 28 GeV. By contrast, the range ratio of Ga nuclides exhibits a much steeper decrease between 1 and 11.5 GeV and closely parallels the behavior of the Sr nuclides. The well known difference at multi-GeV energies in the magnitude of the ranges of neutron-deficient and neutron-excessive products lying in the fission region thus extends to the Ga isotopes but is virtually no longer present for Sc nuclides.

A fruitful way to compare the recoil behavior of different products is in terms of their momenta. Cumming and his collaborators[30-32] have systematized a large number of recoil measurements in this fashion. The present availability of more complete data makes it worthwhile to reexamine in this manner the energy dependence of recoil properties of various types of products. Figure 5 shows the results obtained for ^{91}Sr, a typical fission product, ^{83}Sr, a deep spallation product, ^{24}Na and ^{28}Mg, typical fragmentation products, and $^{44}Sc^{m}$, ^{48}Sc, and ^{67}Cu, which bridge the gap between the fission or deep spallation and the fragmentation mass regions. The various curves are smoothened representations of the present results as well as of published data[1,9,16,29,33,40]. For the sake of consistency the latter were reanalyzed with Cumming's range-energy relation[22]. In performing this calculation we estimated the effective charge of cumulatively formed products on the basis of published charge dispersion data[6,16,34-38].

The various curves in Fig. 5 indicate that products with $A \leq 100$ may be grouped into a number of categories on the basis of the variation with energy of their momenta. The simplest and best understood behavior is that of fission products, such as ^{91}Sr. Provided that the mass division is not too asymmetric their mean momentum at 450 MeV is 130-135 $(MeV\text{-}amu)^{\frac{1}{2}}$ and it decreases by at most 3-4% as the proton energy is increased to 300 GeV. Neutron deficient products in the fission mass region, such as ^{83}Sr, exhibit a completely different behavior. At low energies their momentum has a value that is typical of fission products. However, between ∿ 1 and 10 GeV the momentum decreases substantially as the dominant mechanism changes from fission to deep spallation. The momentum of ^{67}Cu is reasonably high at low energies and its energy dependence is intermediate to that

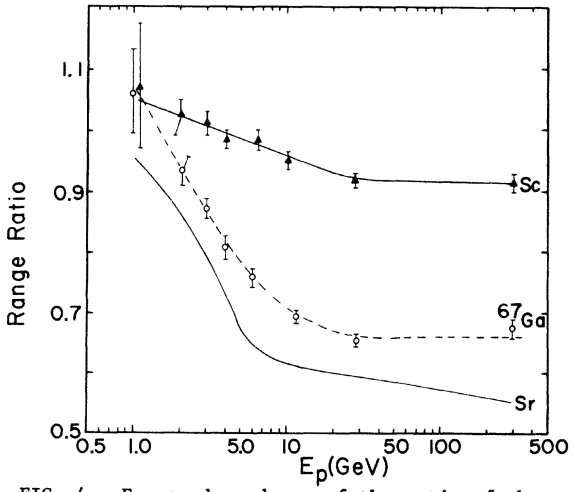

FIG. 4. Energy dependence of the ratio of the experimental range of $^{44}Sc^{m}$ to that of ^{48}Sc (solid points). The dashed curve through the open points is a similar plot for $^{67}Ga/^{73}Ga$ and the solid curve refers to $^{83}Sr/^{91}Sr$.

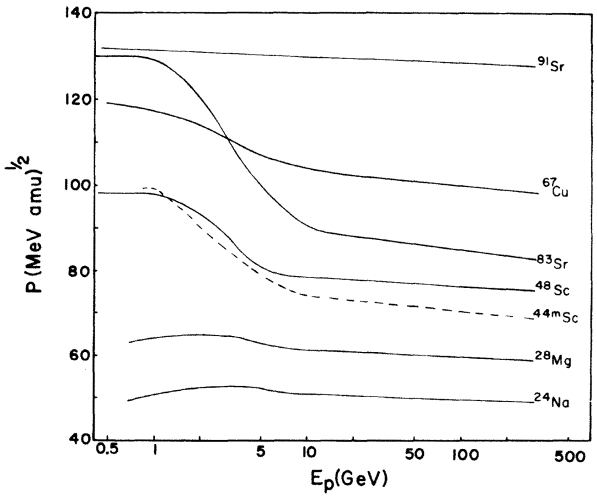

FIG. 5. Energy dependence of the momentum (in the moving system) of various products from the interaction of ^{238}U with high-energy protons.

observed for ^{91}Sr and ^{83}Sr. The range-ratio curve for ^{67}Ga and ^{73}Ga depicted in Fig. 4 suggests that the behavior of neutron deficient isotopes in this mass region should parallel that of ^{83}Sr. The curves for ^{48}Sc or ^{44}Sc^{m} are qualitatively similar to that for ^{83}Sr although, as expected for low-mass products, the magnitude of the momentum is substantially smaller. As already noted above, one important difference between this and the higher mass region is the similarity of the behavior of both neutron-excessive and neutron-deficient products. Finally, the curves for the lightest fragments are once again qualitatively different in that their momentum is nearly independent of bombarding energy. It thus appears that all neutron deficient products, from those lying in the fission mass region down to ^{44}Sc^{m} exhibit a substantial decrease in momentum between 1 and 10 GeV. By contrast, the behavior of neutron excessive products is more complex. Both fission products and light fragments have nearly constant momenta at all energies while products in the intermediate mass region exhibit, to a greater or lesser extent, a transition from high to low momentum.

Having considered the energy dependence of the momentum of various types of products we now turn more specifically to the mass dependence at energies below ($\leq$ 1 GeV) and above ($\sim$ 11.5 GeV) the transition region. A useful way to systematize these data is to assume that the various products arise from a two-body breakup process and determine the extent to which their momenta are consistent with the breakup of a given nucleus. The momenta of fragments resulting from a two-body breakup process may be calculated by means of the liquid drop model of overlapping spheroids developed by Nix and Swiatecki[39] for comparison with low-energy fission data. The results for neutron excessive products are shown in Figure 6 and those for neutron deficient products in Figure 7, where the experimental momenta[1,5,6,9,16,33,40] are compared with the values calculated for various fissioning nuclei[41]. ^{234}U and ^{203}Bi have previously[30] been used in calculations of this type as representative fissioning nuclei for processes involving either low or high deposition energies in the interaction of ^{238}U with 0.45 or 1.8 GeV protons. ^{174}Ta is typical of fissioning nuclei resulting from the still higher deposition energies that may be attained at high bombarding energies. The choices of ^{152}Tb or ^{129}Ba as fissioning nuclei, while perhaps beyond the limit of credibility, are based on the fact that some of the data seem to require such low Z progenitors. It should be emphasized that agreement with a given curve should not be taken to mean that the production mechanism necessarily is either binary fission or even some less restrictive type of two-body breakup process but merely that the results are consistent with such a process. It must also be noted that the calculated curves yield the momenta of primary fragments while the observed products are presumably formed after some additional post-fission evaporation. Since evaporation involves a reduction in both mass and momentum its occurrence will, to first order, merely move the points along a given curve without significantly changing the identity of the presumed fissioning nucleus.

Having made these prefatory comments let us proceed to the comparison between experiment and calculation. Consider first the neutron excessive products. The momenta obtained at low energies are consistent with a ^{234}U fissioning nucleus for products as light as ^{67}Cu. The momenta of lighter products rapidly drop relative to the calculated

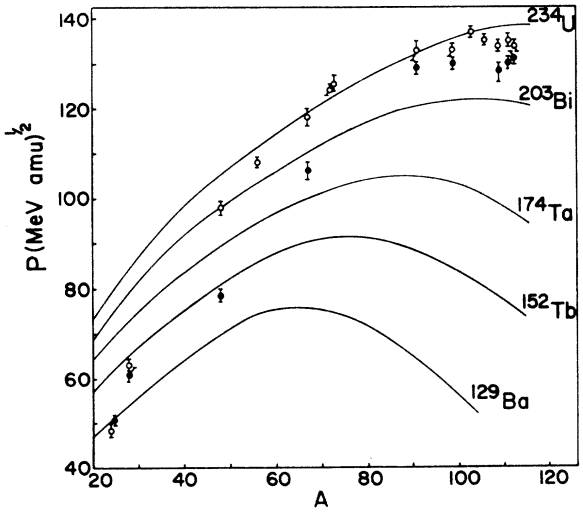

FIG. 6. Mass dependence of the momentum of neutron excessive products formed in the interaction of ^{238}U with 11.5 (closed points) or 0.45-0.7 (open points) GeV protons. The curves represent the momenta predicted by the liquid drop model[39] for the indicated fissioning nuclei.

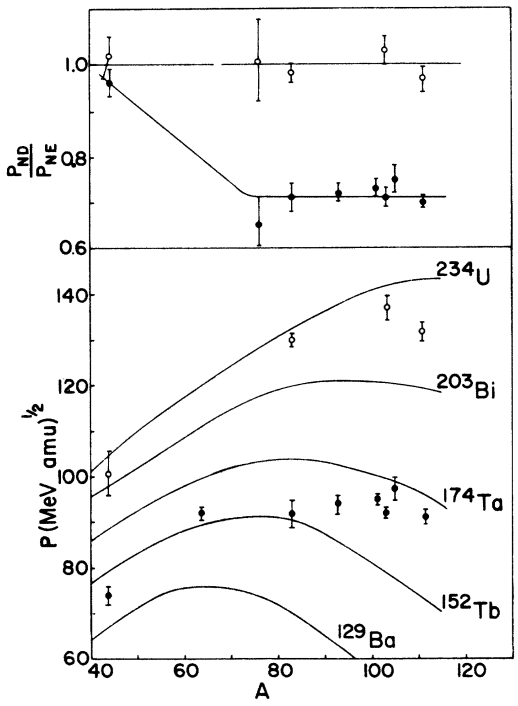

FIG. 7. Bottom panel - mass dependence of the momentum of neutron deficient products formed in the interaction of ^{238}U with 11.5 (closed points) or 0.45-1 (open points) GeV protons. The curves have the same meaning as in Fig. 6. Top panel - Ratio of momenta of isotopic neutron-deficient and neutron-excessive products at 0.45-1 (open points) or 11.5-18 (closed points) GeV.

values and those of the lightest fragments are only consistent with the lightest of the putative fissioning nuclei[42]. The behavior is qualitatively similar at high energies except that the deviations from the values expected for a heavy fissioning nucleus already manifest themselves for ^{67}Cu. A less significant but apparently real difference is that even products in the fission region require a fissioning nucleus of somewhat lower charge and mass than ^{234}U.

The data on neutron-deficient products are not as abundant, particularly at low energies. The latter are nonetheless consistent with a ^{234}U fissioning nucleus although the uncertainty in the ^{44}Sc^{m} datum is too large to distinguish between a ^{234}U or a ^{203}Bi parent. It may thus be concluded that below 1 GeV both neutron-excessive and neutron-deficient products with A $\gtrsim$ 65 are consistent with the fission of ^{234}U. This similarity between these two types of products is also displayed in the top panel of Figure 7 which shows the ratio of momenta of neutron-deficient to neutron-excessive isotopes of a given element. The low-energy ratios are thus seen to be consistent with unity over the entire range of plotted A values.

The situation is dramatically different at high energies. The momenta of neutron-deficient products are now consistent with fissioning nuclei ranging from ^{174}Ta for nuclides in the fission product region to one just slightly more massive than ^{129}Ba for the lightest fragment. The momentum ratio curve shows that the momenta of neutron-deficient products are some 30% smaller than those of neighboring neutron-excessive ones down to at least A $\sim$ 75.

It may be concluded that if all the products in question are formed in a fission-like process the fissioning nucleus, according to the model of Nix and Swiatecki[39], ranges from ^{234}U for fission products down to ^{129}Ba for light fragments. We must, however, add the cautionary note that the spheroid model was not developed for the consideration of binary processes as asymmetric as those leading to the formation of fragments such as ^{24}Na so that the conclusions pertaining to these fragments should perhaps not be taken too seriously. It must also be emphasized that the comparison has been restricted to average momenta. A similar comparison of energy or momentum spectra would be considerably more informative both in terms of a more stringent comparison with the spheroid model and also as an indication of the possible presence of components in the spectra that are clearly inconsistent with binary division. This would require either differential range studies at high energies[8,30,31] or direct determinations of the energy spectra of fragments. Experiments of the latter type have been performed[43,44] but complete data are only available for lighter fragments than those of present interest.

B. Cross-sections, F/B Values and Momenta of the Struck Nuclei

The excitation functions for the formation of Sc nuclides, Figure 1, are characteristic of products requiring high deposition energies for their formation. The cross sections thus increase steeply with energy and level off at $\sim$ 10 GeV. Although the cross sections at 11.5 GeV are uniformly higher than those at 28.5- or 300 GeV, pointing to the occurrence of peaks in the excitation functions, the differences are only marginally significant. The weighted average value of $\sigma_{300}/\sigma_{11.5}$ for all four Sc nuclides thus is 0.92±.07, in general agreement with the results of other recent determinations[29,45,46] at these energies. While we are unable to make any detailed comments about the isotopic yield distribution it is apparent that there is a gradual shift in yield towards lower neutron number with increasing energy. This is perhaps most easily demonstrated in Fig. 1 by the fact that the excitation function of ^{46}Sc first crosses that of ^{48}Sc and then that of ^{47}Sc.

The F/B values display a rather striking energy dependence as shown in Figure 3. The F/B initially increase with bombarding energy, peak at about 3 GeV, and then decrease to a value very close to unity at 300 GeV. The peak appears to be somewhat more pronounced for ^{44}Sc^{m} than for ^{48}Sc but at the highest energies the values are essentially the same for all the isotopes. The qualitative features of this plot are similar to those previously determined for other products requiring high deposition energies for their formation such as ^{131}Ba, ^{83}Sr, ^{28}Mg and ^{24}Na [refs. 1,9]. What is remarkably unique about the Sc products is that F/B decreases to a value as low as unity at 300 GeV. Recent measurements by the Argonne group[47] on products in this mass region from the interaction of gold with 300 GeV protons yield similar results. Since F/B is a measure of the forward momentum imparted to the struck nucleus in the initial interaction this result suggests that at the highest energies the struck nuclei which eventually form Sc products acquire virtually no forward momentum.

In order to ascertain whether the energy dependence of F/B can be understood within the context of the conventional model of high-energy nuclear reactions we have used a combination of two simple models to attempt to reproduce the observed behavior. Porile and Sugarman[48] showed that the shapes of excitation functions for the formation of high-energy reaction products could be explained on the assumption that a given product requires a moderately narrow range of deposition energies for its formation. The average deposition energy obtained from recoil studies is thus expected to increase with bombarding energy until there is a good overlap between the deposition energy required for the formation of the product in question and the most probable deposition energy of the struck nucleus. Beyond this bombarding energy the deposition energy should remain essentially constant. Turkevich[49] proposed a simple kinematic model relating the momentum of a struck nucleus to its deposition energy. According to this model the intranuclear cascade may be represented by an elastic collision between the incident proton and one of the target nucleons. The incident proton escapes from the nucleus while the struck nucleon is captured and its kinetic energy and momentum become the deposition energy and momentum of the struck nucleus. In spite of its simplicity this model has been successfully used to account for the energy dependence of recoil properties[50]. It also yields a relation between the forward momentum of a struck nucleus and its deposition energy that agrees well with that obtained from Monte Carlo cascade calculations[21,24].

We assume that the deposition energy for the formation of a given product varies with energy in the manner suggested by Porile and Sugarman[48] and use Eq. (4), which is consistent with the Turkevich model provided k = 1, to obtain $v_{\parallel}$. The latter are then combined with the experimental values of V in order to obtain F/B values by means of Eq. (3). As shown in Table VI, the actual depo-

sition energies do indeed initially increase with bombarding energy. However instead of levelling off the E^* values go through a peak, an effect that is presumed to arise from a breakdown in the model. We have used the experimental values of E^* as long as this quantity increases with energy and the maximum value at higher energies.

We have performed this calculation for all high deposition-energy products from ^{238}U for which recoil data are available as a function of energy. Figure 8 presents the calculated and experimental[1,9,33,45] results for ^{24}Na, $^{44}Sc^m$, and ^{131}Ba, which are typical of all the available data. Several features of this comparison are worthy of note. First of all it must be stated that the agreement between experiment and calculation up to the peak energy is a necessary consequence of the use of Eq. (4) with k=1. Of greater interest is the fact that the calculation does indeed predict the occurrence of peaks in the F/B values at the correct energies. However these peaks are considerably less pronounced than the experimental ones and the curves rapidly level off while the measured values continue to decrease up to 300 GeV. The shape of the calculated curves is simply a consequence of the fact that, for a given excitation energy transfer, the momentum imparted to the struck nucleus is proportional to the ratio of the momentum of the incident proton to its kinetic energy. At nonrelativistic energies this ratio varies as $T_p^{-1/2}$ and so F/B, which is a measure of the forward momentum of the struck nucleus, decreases with increasing proton energy. On the other hand, at highly relativistic energies this ratio is independent of T_p and in this energy domain F/B becomes invariant. Since the maximum E^* values are attained at bombarding energies of a few GeV, the calculated F/B do show some decrease but rapidly flatten out with increasing energy. This trend is accelerated by the concomitant decrease in the kinetic energy of the fragments which, for a given $v_{\parallel}$, results in higher values of $\eta_{\parallel}$ and so of F/B. The curve for ^{24}Na, whose range above 3 GeV decreases to a much smaller extent than those of the other products, features a more gradual levelling off. The discrepancy between experiment and calculation thus indicates that the data are inconsistent with an analysis based on a conventional model of high-energy reactions and confirms from a slightly different point of view the breakdown of the relation between forward momentum and deposition energy.

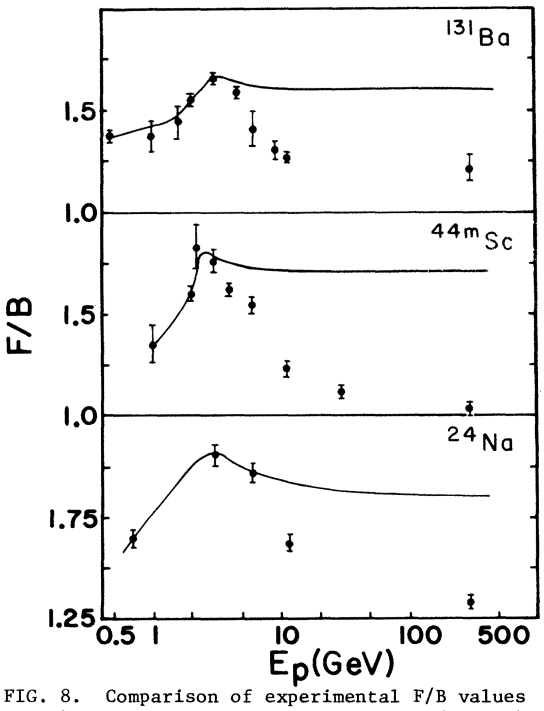

FIG. 8. Comparison of experimental F/B values (points) with 2-nucleon collision model (curves).

Considerable evidence has accumulated in recent years to suggest that the relativistic secondary particles resulting from the interaction of an ultra-relativistic proton with a complex nucleus escape from the nucleus without undergoing significant interaction. The close agreement between the mass-yield curves measured at 11.5 and 300 GeV for a variety of targets[51-53] indicates that the deposition energy spectrum remains essentially unchanged. Similar evidence has been obtained in emulsion studies[54] showing that the number of heavy prongs is virtually independent of energy over nearly the same energy range. However it has also been found that the number of shower particles (mostly pions) does increase substantially over the above energy range[54,55]. Since pions are usually considered to be efficient in transferring excitation energy to the nucleus these two sets of observations can only be reconciled on the assumption that in ultra-relativistic reactions the shower particles do not participate in the intranuclear cascade. The energy flux model proposed by Gottfried[56] accounts for this assumption. According to this model the hadron state produced in the initial interaction of an ultra-relativistic proton is sufficiently long-lived in the target rest frame to have a reasonably high probability of escaping from the nucleus prior to decaying to its final multi-particle state.

This picture of high-energy reactions can readily be incorporated into the two-nucleon collision model. We merely replace the elastic collision between the incident proton and a target nucleon by an inelastic collision in which the emitted particle is an excited hadron of mass m^*. The ratio of m^* to the proton rest mass is given by the relation

$$\frac{m^*}{m_p} = \frac{T_p + E^* + T_p E^* - 3.253\times10^{-2} A_T v_{\parallel} (T_p^2+2T_p)^{1/2}}{T_p - E^*} \qquad (5)$$

where the various quantities have the same meaning as in Eq. (4).[61] The appropriate E^* value for high bombarding energies is the maximum value obtained from recoil data in the vicinity of 3 GeV. At lower energies, where the elastic two-nucleon collision model constitutes a reasonable approximation, m^*/m_p reduces to unity as can be seen by inserting E^* from Eq. (4) (with k=1) into Eq. (5).

We have analyzed the recoil data displayed in Fig. 8 with this effective mass formulation and show the values of m^*/m_p in Fig. 9. The mass ratio begins to increase above unity between 2 and 6 GeV and levels off at values ranging from 1.3 to 2.3 at the highest energies. While it is apparent that the highest m^* values are obtained for high deposition-energy products having very low F/B, the data are too sparse to permit a detailed systematization of m^* values. At any rate, it is clear that the emission of excited hadrons in the cascade provides a reasonable mechanism for the

formation of residual nuclei having high excitation energy but low forward momentum and can thus account for a heretofore puzzling feature of high-energy nuclear reactions. It will be of interest to see whether Monte Carlo cascade calculations incorporating this feature will be able to reproduce this result.

The F/B ratios may be examined from a somewhat different viewpoint. The two-nucleon collision model relates the kinematic quantities discussed above to the angles through which the incident proton and the struck nucleon are scattered, denoted by ψ and θ, respectively. For a given E^* value, ψ and θ may be determined. The angle θ is of particular interest since, within the framework of the model, it establishes the direction relative to the beam at which the struck nucleus recoils as a result of its interaction with the incident proton. Its value is given by

$$\theta = \tan^{-1}\left[\frac{2T_p}{E^*(T_p+2)} - 1\right]^{1/2}. \qquad (6)$$

The values of θ consistent with the recoil data may be obtained by use of the experimentally determined deposition energies. Alternatively, the maximum E^* values may be used in conjunction with the appropriate m^* in a somewhat different expression to obtain the same results. Figure 10 shows a typical θ curve, that consistent with the recoil properties of ^{48}Sc. It is seen that θ remains nearly constant between 0.45 and 3 GeV and then rapidly increases with energy, attaining a value of $\sim 80°$ at 300 GeV. Evidently, at high energies the direction of motion of the captured nucleon is nearly transverse to that of the incident proton. The importance of transverse momentum transfer in interactions in which little forward momentum is imparted to the struck nucleus has been previously deduced[24] from an analysis of Monte Carlo cascade calculations. This situation is also reminiscent of that considered by Halpern[57] in his explanation of the occurrence of sideways peaking in the angular distribution of fission products at high energies. He pointed out the importance at these energies of interactions such as those considered in the two-nucleon collision model which result in the capture of a low-energy nucleon moving in a direction perpendicular to that of the beam. The result of such a collision is similar to that obtained in the bombardment with a low-energy projectile moving perpendicular to the beam direction. Since the angular momentum of the struck nucleus is now oriented in a plane parallel to the beam the angular distribution of the products peaks at 90°. Monte Carlo cascade calculations[58] at 0.4 GeV confirm[30] that the angular momentum of residual nuclei having low E^* is preferentially directed along the beam axis.

An equivalent interpretation of the data in Figure 10 may be given in terms of the velocity vector model of high-energy reactions. If the intra-nuclear cascade is approximated by the two-nucleon collision model then $\tan\theta = \eta_\perp/\eta_\parallel$, where $\eta_\perp = v_\perp/V$ and $v_\perp$ is the transverse component of the cascade velocity v. The θ curve for ^{48}Sc formation then indicates that with increasing bombarding energy the value of $\eta_\perp/\eta_\parallel$ increases from ~ 0.5 to 5. A change of this magnitude, coupled with the expected change in the angular momentum orientation, has interesting implications for the angular distribution of the emitted fragments. It is easy to show that under these conditions the angular distribution should change from one peaking at forward angles when $\eta_\perp/\eta_\parallel \lesssim 1$ to one peaking sideways when $\eta_\perp/\eta_\parallel \gg 1$. Remsberg and Perry[44] have recently measured the angular distribution of light fragments emitted in the interaction of heavy elements with 28 GeV protons. They find that the differential cross sections peak in the vicinity of 90°, in marked contrast to the forward peaking obtained at lower energies[8]. This result is in accord with the above considerations and we expect on this basis that sideways peaking should be even more pronounced at 300 than at 28 GeV[59]. One possible mechanism for sideward peaking is the occurrence of a collective excitation. Glassgold, Heckrotte, and Watson[60] suggested that a very high-energy proton might initiate a shock wave along its path in the struck nucleus because of the narrow cone to which the fast secondaries are confined. The shock wave would be propagated through the nucleus at an angle of $\sim 80°$ to the beam direction and might lead to the eventual emission of fragments at large angles. More detailed experiments at 300 GeV are obviously needed before any conclusions can be drawn.

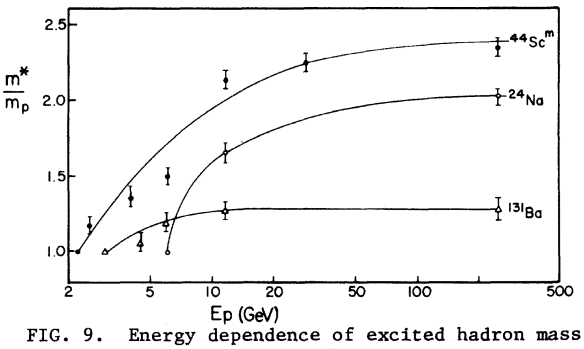

FIG. 9. Energy dependence of excited hadron mass (in terms of proton rest mass) consistent with data in Fig. 8 as obtained from inelastic 2-nucleon collision model.

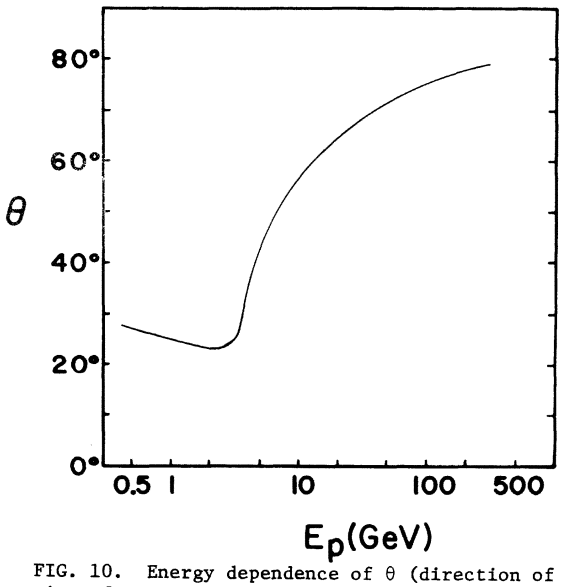

FIG. 10. Energy dependence of θ (direction of motion of struck nucleus relative to beam) according to 2-nucleon collision model as obtained from ^{48}Sc data.

As stated in the Introduction the research described in this article was partly motivated by the energy dependence of the recoil properties of deep spallation products. Beg and Porile[1] were able to account for both the range and F/B ratio of ^{131}Ba above the transition energy by means of a cascade-evaporation calculation modified to include the emission of ^{24}Na. This fragment was assumed to be emitted in the course of the cascade with an energy and angular distribution characteristic of 2.9 GeV proton bombardment of bismuth[8]. We have already noted that recent measurements[9,44] show that while the energies of light fragments do not change substantially above 3 GeV the F/B ratios decrease markedly reflecting the change in the angular distribution from forward to sideways peaking. It thus becomes of interest to determine the extent to which ^{24}Na fragments having the properties determined at 28 GeV[44] can account for the recoil properties of ^{131}Ba at high energies. We restrict ourselves to a consideration of the F/B value since the range of ^{131}Ba will not be significantly altered by the change in the angular distribution of a ^{24}Na partner.

The energy dependence of F/B for ^{131}Ba is shown in Fig. 8. The maximum value of F/B occurs at 3 GeV and corresponds to $v_{\parallel} = 0.0723$ (MeV/amu)$^{1/2}$. According to the two-nucleon collision model a constant deposition energy above 3 GeV would reduce this value to 0.0613 at 11.5 GeV corresponding to an expected F/B value of 1.65. The measured[1] F/B at this energy is 1.27. Let us estimate the effect on the expected value of $v_{\parallel}$ of a ^{24}Na fragment emitted in the cascade with velocities and differential cross section at each angle given by the measured laboratory distributions. The mean value of the velocity component of ^{24}Na along the beam direction may be estimated as

$$v_{\parallel}(^{24}\mathrm{Na}) = \frac{\int_0^{\pi} W(\theta)\,\bar{V}(\theta)\cos\theta\sin\theta\,d\theta}{\int_0^{\pi} W(\theta)\sin\theta\,d\theta} \qquad (7)$$

where $W(\theta)$ is the relative number of fragments per unit solid angle emitted at laboratory angle θ and $\bar{V}(\theta)$ is the mean velocity of fragments emitted at this angle. The component along the beam direction of the velocity acquired by the residual nucleus as a result of fragment emission $v_{\parallel}$ (frag) may be obtained by momentum conservation as $v_{\parallel\,\mathrm{frag}} = -24v_{\parallel}(^{24}\mathrm{Na})/M_R$ where we have chosen $M_R = 210$ corresponding to fragment emission from ^{234}U. The net velocity of the residual nucleus formed in 11.5 GeV proton bombardment thus becomes 0.0613 + $v_{\parallel\,\mathrm{frag}}$. This quantity may be combined with the experimental value of V for ^{131}Ba, 0.617 (MeV/amu)$^{1/2}$, to yield a value of $\eta_{\parallel}$ which may be inserted in Eq. (3) for the determination of F/B.

We have performed this calculation for both the ^{24}Na distribution obtained at 2.9 GeV[8], where the velocities were increased by a factor of 1.05 to make them applicable to ^{238}U instead of ^{209}Bi, and that determined at 28 GeV[44,61]. The former yields F/B = 1.21 and the latter F/B = 1.38. Although the higher-energy fragment data yield a somewhat higher F/B ratio than the experimental value of 1.27 there is still a substantial reduction from the value of 1.65 which would be expected in the absence of prompt fragment emission. It thus appears that fragmentation can still qualitatively account for the properties of deep spallation products in spite of the seemingly different nature of this process at very high energies. The effect of fragment emission in reducing the value of $v_{\parallel}$ thus is qualitatively similar to that caused by the emission of an excited hadron and it may be that both effects are of importance.

V. CONCLUSIONS

The present results on Sc nuclides formed in the interaction of ^{238}U with high-energy protons coupled with previous measurements on other products permit some general conclusions to be drawn concerning the formation of fragments and deep spallation products. It appears that the F/B ratios of products requiring high deposition energies for their formation peak in the vicinity of 3 GeV. While the occurrence of this peak can be understood on kinematic grounds the continuing decrease of F/B at higher energies can only be explained within the framework of the conventional two-step model of high-energy reactions on the assumption that a highly excited energetic hadron is emitted from the struck nucleus in the forward direction. An alternative explanation for the low F/B values may lie in the fact that the collisions leading to the products of interest appear to be associated with relatively high transverse momentum transfer to the struck nucleus. This effect may possibly be associated with some collective phenomenon such as a shock wave and the fragmentation process at ultra-relativistic energies may perhaps be explainable in these terms. Clearly, more detailed experiments at high energies are needed to test these various ideas.

The energy dependence of the momentum of fragments having $A \lesssim 100$ points to a variety of processes. It appears that the momentum of all neutron-deficient products decreases sharply between 1 and 10 GeV and shows little variation outside this interval. On the other hand, neutron-excessive fission products and light fragments have momenta that vary little with energy while products of intermediate mass are in this respect akin to the neutron-deficient fragments. The precise delineation between these three mass regions awaits the availability of data on more fragments. An analysis of all the available data in terms of the liquid drop model indicates that the data are consistent with the binary division of nuclei ranging from ^{234}U in the case of fission products to ^{129}Ba for light fragments.

The continued assistance of Dr. E. P. Steinberg with the ZGS bombardments is gratefully appreciated. We wish to thank Ms. E. M. Franz for her help with the AGS irradiations and Dr. M. W. Weisfield for his assistance in performing the FNAL bombardments.

---

*Work supported by the U.S. Energy Research and Development Administration.

†Present address: Department of Chemistry, University of Oslo, Oslo, Norway.

[1] K. Beg and N. T. Porile, Phys. Rev. C3, 1631 (1971).

[2] J. Alexander, C. Baltzinger, and M. F. Gadzik, Phys. Rev. 129, 1826 (1963).

[3] R. Brandt, in "Proceedings of the Symposium on the Physics and Chemistry of Fission, Salzburg, 1965" (International Atomic Energy Agency, Vienna, Austria, 1965), Vol. 2, p. 329.

[4] E. Hagebø and H. Ravn, J. Inorg. Nucl. Chem. 31,

2649 (1969).
[5]J. A. Panontin and N. T. Porile, J. Inorg. Nucl. Chem. 30, 2027 (1968).
[6]J. A. Panontin and N. T. Porile, J. Inorg. Nucl. Chem. 32, 1775 (1970).
[7]E. Hagebø, J. Inorg. Nucl. Chem. 32, 2489 (1970).
[8]J. B. Cumming, R. J. Cross, J. Hudis, and A. M. Poskanzer, Phys. Rev. 134, B167 (1964).
[9]S. B. Kaufman and M. W. Weisfield, Phys. Rev. C11, 1258 (1975).
[10]Y. W. Yu and N. T. Porile, Phys. Rev. C7, 1597(1973)
[11]Y. W. Yu and N. T. Porile, Phys. Rev. C12, 938(1975)
[12]The Radiochemistry of Scandium (NAS-NS 3020), Nuclear Science Series, National Academy of Sciences - National Research Council.
[13]J. T. Routti and S. G. Prussin, Nucl. Instr. 72, 125 (1969).
[14]J. Tobailem, C. de Lassus St. Genies, and L. Leveque, Centre d'Etudes Nucleaires de Saclay Report CEA-N-1466(1), 1971 (unpublished); J. B. Cumming, Annu. Rev. Nucl. Sci. 13, 261 (1963).
[15]S. B. Kaufman, M. W. Weisfield, B. D. Wilkins, D. Henderson, and E. P. Steinberg, Phys. Rev. C13, 253 (1976).
[16]N. Sugarman, H. Münzel, J. A. Panontin, K. Wielgoz, M. V. Ramaniah, G. Lange, and E. Lopez-Menchero, Phys. Rev. 143, 952 (1966).
[17]G. Friedlander and L. Yaffe, Phys. Rev. 117, 578 (1960).
[18]Y. Y. Chu, (private communication).
[19]H. Ravn, J. Inorg. Nucl. Chem. 31, 1883 (1969).
[20]N. Sugarman, M. Campos, and K. Wielgoz, Phys. Rev. 101, 388 (1956).
[21]N. T. Porile and N. Sugarman, Phys. Rev. 107, 1410 (1957).
[22]J. B. Cumming (private communication).
[23]L. C. Northcliffe and R. F. Schilling, Nucl. Data A7, 233 (1970).
[24]N. T. Porile, Phys. Rev. 120, 572 (1960).
[25]N. Metropolis, R. Bivins, M. Storm, J. M. Miller, G. Friedlander, and A. Turkevich, Phys, Rev. 110, 204 (1957).
[26]J. M. Alexander, in "Nuclear Chemistry," edited by L. Yaffe (Academic, New York, 1968), Vol. I, p. 273.
[27]N. T. Porile, Phys. Rev. 185, 1371 (1969).
[28]The gallium results were obtained in the present study but the data suffered from 20-30% uncertainties and so are not separately presented. However the ratio of the ranges of various gallium nuclides could be determined to an accuracy of ∿ 5%.
[29]S. K. Chang and N. Sugarman, Phys. Rev. C9, 1138 (1974).
[30]V. P. Crespo, J. B. Cumming, and A. M. Poskanzer, Phys. Rev. 174, 1455 (1968).
[31]K. Bächmann and J. B. Cumming, Phys. Rev. C5, 210 (1972).
[32]J. B. Cumming and K. Bächmann, Phys. Rev. C6, 1362 (1972).
[33]V. P. Crespo, J. M. Alexander, and E. K. Hyde, Phys. Rev. 131, 1765 (1963).
[34]S. Kaufman, Phys. Rev. 129, 1866 (1963).
[35]G. Friedlander, in "Proceedings of the Symposium on the Physics and Chemistry of Fission," Salzburg, 1965 (International Atomic Energy Agency, Vienna, Austria, 1965), Vol. 2, p 265.
[36]N. T. Porile, Phys. Rev. 148, 1235 (1966).
[37]J. Hudis, Phys. Rev. 171, 1301 (1968).
[38]J. A. Panontin and N. T. Porile, J. Inorg. Nucl. Chem. 30, 2017 (1968).
[39]J. R. Nix and W. J. Swiatecki, Nucl. Phys. 71, 1 (1965).
[40]S. K. Chang and N. Sugarman, Phys. Rev. C8, 775 (1973).
[41]The calculation is based on a numerical integration of Eq. 48 in ref. 39 and includes the effect of anharmonicity of the potential energy. In addition, the calculated data were corrected for the difference between the charge-to-mass ratio of the observed fragment and that of the assumed fissioning nucleus.
[42]In a previous analysis of recoil data for a ^{238}U target obtained at 0.4-0.7 GeV Crespo et al. (ref. 30) concluded that all products down to ^{24}Na were consistent with a ^{234}U fissioning nucleus. The difference from the present conclusion for light fragments is that these authors used an approximation that is not valid for very asymmetric divisions.
[43]A. M. Poskanzer, G. W. Butler, and E. K. Hyde, Phys. Rev. C3, 882 (1971).
[44]L. P. Remsberg and D. G. Perry, Phys. Rev. Lett. 35, 361 (1975).
[45]Y. W. Yu and N. T. Porile, Phys. Rev. C10, 167 (1974).
[46]Y. W. Yu, S. Biswas, and N. T. Porile, Phys. Rev. C11, 2111 (1975).
[47]S. B. Kaufman, private communication.
[48]N. T. Porile and N. Sugarman, Phys. Rev. 107, 1422 (1957).
[49]A. Turkevich, quoted in ref. 21.
[50]A. M. Poskanzer, J. B. Cumming, and R. Wolfgang, Phys. Rev. 129, 374 (1963).
[51]S. Katcoff, S. B. Kaufman, E. P. Steinberg, M. W. Weisfield, and B. D. Wilkins, Phys. Rev. Lett. 30, 1221 (1973).
[52]G. English, Y. W. Yu, and N. T. Porile, Phys. Rev. Lett. 31, 244 (1973).
[53]G. English, Y. W. Yu, and N. T. Porile, Phys. Rev. C10, 2281 (1974).
[54]Barcelona-Batavia-Belgrade-Bucharest-Lund-Lyon-Montreal-Nancy-Ottawa-Paris-Rome-Strasbourg-Valencia Collaboration, Phys. Lett. 48B, 467 (1974).
[55]F. T. Dao, D. Gordon, J. Lach, E. Malamud, T. Meyer, and R. Poster, Phys. Rev. Lett. 29, 1627 (1972).
[56]K. Gottfried, Phys. Rev. Lett. 32, 957 (1974).
[57]I. Halpern, Nucl. Phys. 11, 522 (1959).
[58]K. Chen, Z. Fraenkel, G. Friedlander, J. R. Grover, J. M. Miller, and Y. Shimamoto, Phys. Rev. 166, 949 (1968).
[59]The values of E^* were obtained by means of an analysis (Eqs. 2 and 3) in which it is assumed that $\eta_\perp = 0$ and that the angular distribution of V is isotropic. The occurrence of sideways peaking has very little effect on this analysis and, in fact, leads to even lower E^*. For instance E^* for ^{48}Sc formation at 300 GeV is reduced from 72 to 66 MeV for $\eta_\perp = 5\eta_\parallel$ and an angular distribution of V of the form $W(\theta) = 1 - 0.5 \cos^2\theta$.
[60]A. E. Glassgold, W. Heckrotte, and K. M. Watson, Ann. Phys. (New York) 6, 1 (1959).
[61]The use of an inelastic collision model to analyze recoil data was introduced by L. Winsberg [Phys. Rev. 135, B1105 (1964)] and J. B. Cumming [Phys. Rev. 137, B848 (1965)] and was successfully applied to the $(p,p\pi^+)$ reaction by L. P. Remsberg [Phys. Rev. 138, B572 (1965)] and by Poskanzer, Cumming and Remsberg [Phys. Rev. 168, 1331 (1968)]. Our formulation differs from these earlier approaches in that we assume that the excess mass i.e. $(m^*-m_p)/m_p$ is negligibly small compared to the bombarding energy T_p, an approximation that becomes particularly valid at the highest energies of interest.